FRACTURE TOUGHNESS OF STRUCTURAL COMPONENTS. INFLUENCE OF CONSTRAINTS

Andrzej Neimitz, Jaroslaw Galkiewicz
Kielce University of Technology
Al.1000-lecia PP 7
25-314 Kielce, Poland
neimitz@tu.kielce.pl, jgalka@tu.kielce.pl

Abstract

In the paper the influence of the in- and out-of-plane constraint on fracture toughness was analyzed theoretically and experimentally. It was assumed that the *Q* stress is a measure of in-plane constraint and Guo's *Tz* function is a measure of out-of-plane constraint. The general formula was proposed to compute the fracture toughness when two or more fracture mechanisms are active in parallel and they are represented by their individual fracture toughness'. The simple, analytical formulas were derived to compute fracture toughness' for different fracture mechanisms acting individually. They are functions of three parameters: J_{IC}, *Q*, *Tm*. Experimental program was carried out to measure fracture toughness of the *specimen*, J_c. 2D and 3D FE analysis was performed to compute all necessary quantities. Theoretical models proved to be correct when compared with the experimental results for tested materials.

Introduction

Due to the high geometrical constraint the fracture toughness measured in the laboratory, according to national or international standards assumes values among the lowest for variety of other geometrical configurations. Therefore, structural integrity assessment procedures using the K_{IC} or J_{IC} or similar toughness measures provide, by definition, conservative results. It is, in principle, correct approach leading to "save" decisions.

However, safety although the most important requirement imposed on structural integrity assessment procedures, is not a unique one. The structure should be not only safe but cheap as well. It turns out, that for structures without high constraint in front of crack the fracture toughness can be several times higher than for specimens with high constraint.

In practice, it is not possible to measure fracture toughness for all structures (different shapes and sizes) made of given material. However, if one could define some measures of constraint (in-plane and out-of plane) computable for different geometries, these measures could be used to propose the physically based formulas defining fracture toughness for arbitrary component.

1. In-plane and out-of-plane constraints measures

1.1. In plane constraint.

For the Ramberg-Osgood (R-O) material the second term of asymptotic expansion of the stress field weakly depends on the distance from the crack tip. O'Dowd and Shih [1] proposed the simplified, two-terms formula for the stress field in front of the crack, in the form:

$$\sigma_{ij}(\theta=0)=\sigma_o\left(\frac{J}{\alpha\varepsilon_o\sigma_o I_n r}\right)^{\frac{1}{1+n}}\tilde{\sigma}_{ij}(\theta,n)+Q\sigma_0\delta_{ij} \qquad (2)$$

where $\varepsilon_o = \sigma_o/E$, n is R-O exponent, I_n is function of n computed for plane strain or plane stress [2].

The Q stress strongly depends on the shape and size of specimen as well as on external loading. It depends also on n and for many cases is considerably different from zero (usually is negative). Thus, the Q stress strongly influences the level of hydrostatic stresses in front of the crack tip. In turn, fracture mechanisms and plastic deformation depend on hydrostatic stresses. One may expect that Q stress can be a good measure of the in-plane constraint.

1.2. Out-of-plane constraint

Guo extended the HRR analysis in a series of papers [3, 4, 5] to the three-dimensional case (3D). In fact, he showed that the HRR singularity can be proven for the plane strain and plane stress only and in 3D case simplified, approximate formula in the form of Eq. (2) (without the second term) in which the thickness effect entered final result through functions *In(n,Tz)* and $\sigma_{ij}(n,\theta,T_z)$. *Tz(n,r,x3)* function is defined as follows:

$$Tz = \frac{\sigma_{33}}{\sigma_{11} + \sigma_{22}} \tag{3}$$

When through-the-thickness average of *Tz*, *Tm* is computed the thickness of the element, *B* enters all important stress and strain characteristics. Importance of this function was demonstrated when it was applied to modify Dugdale model for arbitrary specimen thickness [6]. Similarly to the *Q* stress the *Tz* function can be computed numerically by finite element method or using approximate relations [5].

2. Fracture mechanisms and fracture toughness

Fracture toughness measured experimentally according to appropriate standards depends on dominating fracture mechanisms at or just after onset of crack growth[♣] and on extent of plastic deformation. In this paper fracture during monotonous loading will be discussed. In such a case brittle fracture usually take place according to cleavage, transgranular fracture mechanism. Ductile fracture is due to **v**oids **n**ucleation-**g**rowth-**c**oalescence (VNGC) processes or/and slip along slip facets in two different domains: central part of the specimen in front of the crack and along shear lips. Very often fracture process is a result of more than one fracture mechanism. They can act simultaneously (in parallel) or can follow each other (in series). Usually ductile and cleavage mechanisms do not occur together along crack front. The reason is that cleavage mechanism is stress controlled and take place at very low, if any, plastic deformation. Ductile mechanisms require both high stresses and plastic strains (VNGC) or high plastic strains (slip along slip facets). Ductile fracture mechanisms can occur simultaneously and they do it very often.

In this paper we will postulate that resultant fracture toughness should be computed according to two different schemes:

- one fracture mechanism occurs at or just after onset of crack growth,
- two or more fracture mechanisms occur simultaneously at or just after the onset of crack growth

Former case is observed when cleavage mechanism takes place. The fracture is either by cleavage only or by ductile – cleavage sequence of mechanisms. The scheme depends on actual individual value of fracture toughness associated with cleavage or ductile fracture mechanism considered separately.

[♣] Usually fracture toughness is measured taking into account not only the onset of crack growth (which is difficult to be detected) but some small stable crack growth also (J_R curve technique or 95% secant line).

During ductile fracture different fracture mechanisms can take place at the same time. Examination of fractured specimen surfaces shows that voids are formed along shear lips and in the central part of the specimen. However, shape of cavities in these both domains is different. Along shear lips cavities are elongated, of parabolic shape. Their growth is due to the shearing plastic strain. Shear lips are located near the specimen surfaces in the region dominated by plane stress. In the centre of specimen the shape of cavities is more circular. Plastic strain and hydrostatic stress control their growth. Plane strain or 3D stress and strain dominate this domain. We will assume that fracture mechanisms along shear lips and in the central part of specimen are different and they will be modelled separately. The fracture toughness due to ductile fracture in a central part of specimen will be denoted by J_c^{dv} (VNGC process). The fracture toughness due to mechanisms occurring along shear lips will be denoted by J_c^{ds}. The resultant fracture toughness when two or more mechanisms occur simultaneously will be computed using "electrical" analogy concerning electrical resistance for two or more resistors connected in parallel.

$$\frac{A}{J_c} = \frac{A_v}{J_c^{dv}} + \frac{A_s}{J_c^{ds}} + \ldots \rightarrow J_c = \frac{J_c^{dv} J_c^{ds}}{(A_v / A) J_c^{ds} + (A_s / A) J_c^{dv}} \tag{5}$$

where J_c is resultant fracture toughness, $A=A_v+A_s$ is part of the fractured surface: $A=\Delta aB=(a_1-a_o)B=0.1b_0B$, b_o is length of unfractured ligament in front of the crack, B is specimen thickness, a_o is initial crack length, a_1 is the length of crack after stable crack extension over the distance $0.1b_o$, A_s is part of A- it is the area occupied by shear lips, A_v is part of A occupying central part of selected fractured surface. Crack growth extension equal to $0.1b_o$ was assumed since the value of measured J_{IC} (from the J_R curve) depends on this distance. Areas A, A_v,A_s can be easily measured from the fractured surface.

In order to compute resultant fracture toughness of structural element $J_c(J_{IC},Q,Tm)$ when more than one fracture mechanism occur simultaneously one should compute fracture toughness characteristic for individual fracture mechanisms.

3. Cleavage fracture toughness of structural components

Cleavage, transgranular fracture process is controlled by hoop stress in front of the crack. Since plastic deformations are small, the HRR field (small strains) corrected by the O'Dowd [1] Q stress is a good approximation of "real" stresses in this domain (Eq.(2)). We adopt O'Dowd [7] approach proposing formula to compute fracture toughness. However, we extend his results to include the out-of-plane constraint. Thus, two-parameter approach (J_{IC}, Q), will be replaced by three-parameter approach (J_{IC} , Q, Tz).

O'Dowd assumed [7] that fracture may occur when the hoop stresses reach critical value σ_c at certain distance r_c in front of the crack tip. Assuming that value of J_{IC}, measured according to standards (e.g. ASTM E 1737-96) was obtained for plane strain case (Tz=0.5) for high constraint specimen (Q=0) the critical stresses can be computed from the formula:

$$\sigma_c(\theta = 0, r = r_c) = \sigma_o \left(\frac{J_{IC}}{\alpha \varepsilon_o \sigma_o I_n r_c} \right)^{\frac{1}{1+n}} \tilde{\sigma}_{22}(\theta, n) \tag{6}$$

If specimen is still dominated by plane strain in front of the crack but the in-plane constraint is reduced (Q<0) Eq.(2) can be used, in which J is replaced by J_c, r by r_c, σ_{ij} and $\tilde{\sigma}_{ij}$ by σ_c and $\tilde{\sigma}_{22}$ respectively. Eliminating from Eqs (2) and (6) r_c the following formula for J_c can be reached:

$$J_c = J_{IC}\left(1-\frac{Q}{\sigma_c/\sigma_o}\right)^{1+n} \tag{7}$$

In Eq.(7) J_{IC} should be measured in a standard test, Q should be computed numerically, σ_c is unknown but it can be computed from the simple two tests.

The HRR solution with the second term proposed by O'Dowd does not take into account the thickness effect, except distinction made between plane stress and plane strain. In turn Guo's approximate 3D solution does not take into account in-plane constraint, represented by second, generalised term of asymptotic expansion.

In view of above limitations in representing stress distribution in front of the crack along its edge the following simple, approximate model will be used in computations to follow. The scheme to include *Tz* function into fracture toughness of structural element approximation is shown in Fig. 1.

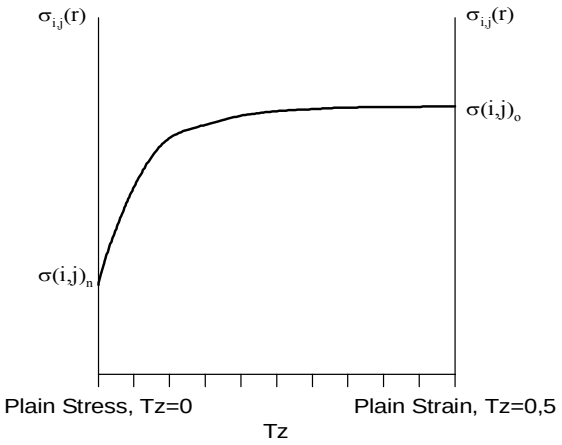

Fig.1. Scheme used to include *Tz* into stress level approximation in front of the crack.

Fig.1 summarises certain known facts as well as assumptions adopted in the process of the stress level approximation for cases which are neither dominated by plane strain nor by plane stress. If *Tz*=0 (plane stress domination) the stress level, $(\sigma_{ij})_n$, can be computed from Eq.(2) with I_n and $\tilde{\sigma}_{ij}(n,\theta)$ functions adopted for plane stress. If *Tz*=0.5 (plane strain domination) the stress level $(\sigma_{ij})_o$ can also be computed from Eq.(2) but with I_n and $\tilde{\sigma}_{ij}(n,\theta)$ functions adopted for plane strain. For 0<*Tz*<0.5 the stress level will be approximated by the power function:

$$\sigma_{ij}(r,Tz,Q) = (\sigma_{ij}(r,Q))_n + \left[(\sigma_{ij}(r,Q))_o - (\sigma_{ij}(r,Q))_n\right]\left(\frac{Tz}{0.5}\right)^{\alpha 1} \tag{8}$$

In our model we will use an average value of *Tz*, *Tm* along the crack front. We will compute it numerically using FE analysis. In all cases *Tm* will be computed at the distance $r=2J/\sigma_o$ from the crack edge.

Exponent $\alpha 1$ should be selected to adjust numerically computed opening stress distribution to postulated distribution according to Eq.(8). However, in order to perform fast structural integrity assessment the value of $\alpha 1$ can be assumed at the level assuring conservative results. For brittle or semi-brittle materials $\alpha 1$ should be selected to be smaller than 0.2.

Utilising O'Dowd hypothesis that at critical moment $\sigma_{22}(\theta=0, r=r_c)=\sigma_c$ along with Eqs (2,6 and 8), for two specimens: standard one (Q=0, Tz=0.5) and not suggested by standard ($Q\neq 0$ and $Tz<0.5$) and eliminating unknown distance r_c one can obtain:

$$J_c = J_{IC}\left\{\left[1-\left(Q_o\left(\frac{Tm}{0.5}\right)^{\alpha 1}+Q_n\left(1-\left(\frac{Tm}{0.5}\right)^{\alpha 1}\right)\right)\left(\frac{\sigma_c}{\sigma_o}\right)^{-1}\right]\left[\left(\frac{Tm}{0.5}\right)^{\alpha 1}+\frac{\xi_n}{\xi_o}\left(1-\left(\frac{Tm}{0.5}\right)^{\alpha 1}\right)\right]^{-1}\right\}^{n+1} \quad (9)$$

where $\xi_{n,o}=\left(\tilde{\sigma}_{22}(\theta=0,n)\left((I_n)^{-\frac{1}{1+n}}\right)\right)_{n,o}$ and subscripts n and o denote plane stress and plane strain respectively. In most practical cases $Q_n\cong 0$. When Tz=0.5 Eq.(9) reduces to Eq.(7)

4. Ductile fracture toughness of structural element due to voids nucleation-growth-coalescence fracture mechanism

We start from VNGC fracture mechanism. The physical nature of this process is totally different than for cleavage fracture. VNGC fracture mechanism is strain and stress controlled. Thus, an approach to assess the fracture toughness should be different.

O'Dowd analysed the in-plane constraint influence on ductile fracture (due to VNGC mechanism) toughness of plane strain specimens [8]. He assumed that the process is strain controlled only and that at the critical moment the crack tip opening displacement (CTOD) reaches critical value, which is material property. He compared CTOD's computed for standard plane strain specimen (Q=0, Tz=0.5) and for specimen for which $Q\neq 0$ and Tz=0.5. In result he obtained:

$$J_c = J_{IC}\frac{d_n(Tz=0.5, Q=0)}{d_n(Tz=0.5, Q\neq 0)} \quad (10)$$

where d_n is function of n only for high constraint specimens. Values of d_n for plane strain or plane stress can be found in any fracture handbook. O'Dowd showed [8, 9] that d_n is also a function of Q-stress when constraint is reduced. However, O'Dowd hypothesis seems to be at least not sufficient to explain experimental observation that fracture toughness increases considerably when specimen thickness is reduced. Moreover, Eq. (10) leads to wrong result if d_n in denominator is replaced by d_n computed for plane stress. Since $(d_n)_n>(d_n)_o$ one would obtain smaller value of J_c for much thinner specimen.

Our arguments to propose formula for J_c, which would include both in- and out-of-plane constraint, are based on analysis of VNGC fracture mechanisms. Crack grows by coalescence with the row of the nearest voids. We assume that, at critical moment, the diameter of void in the cell next to the crack tip is for given material independent of specimen geometry. One can easily integrate McClintock or Rice and Tracy formula to find the radius of void. This radiuses can be compared for two different stress fields in front of the crack, which are characteristic for different constraint. One stress field is characteristic for standard specimen (Tz=0.5, Q=0) the second one reflects arbitrary $Q\neq 0$ and $Tz<0.5$. The strain within the cell was assumed to be proportional to CTOD.

$$J_c^{dv} = J_{IC}\frac{d_n(Tz=0.5,Q=0)}{d_n(Tz<0.5,Q\neq 0)}\frac{\sinh\left[\dfrac{\sqrt{3}\sigma_m(Tz=0.5,Q=0)}{\sigma_0}\right]}{\sinh\left[\dfrac{\sqrt{3}\sigma_m(Tz,Q)}{\sigma_0}\right]} \tag{11}$$

where σ_m is hydrostatic stress in front of the crack, $\sigma_m=(\sigma_{11}+\sigma_{22}+\sigma_{33})/3$, $=(1+Tz)(\sigma_{11}+\sigma_{22})/3$; $d_n(n,Tz=0.5,Q=0) = (d_n)_o$ can be found in any fracture handbook. $d_n(n,Tz<0.5)$ can be computed according to Guo's simplified solution [9]. However, it does not take into account the Q stresses. We propose simple approach here, which follows Guo's results [5] and which is sufficiently accurate for structural integrity assessment. It turns out that $d_n(n,Tz<0.5)$ is almost independent of Tz for $Tz<0.4$ and for this range is almost equal to $(d_n)_n$. Then it smoothly drops to $(d_n)_o$ at $Tz=0.5$. Thus we propose:

$$d_n(Tz,Q) = (d_n)_n\left\{H(0.4-Tm)+\left[1-\left[1-\frac{(d_n(Q))_o}{(d_n)_n}\right]\left(\frac{Tm-0.4}{0.1}\right)^{\beta}\right]H(Tm-0.4)\right\} \tag{12}$$

where $H(-)$ is Heaviside step function and β may be assumed, e.g. $\beta=0.5$ (the value of β does not have essential influence on final result obtained since Tm not often is grater than 0.4).

In Eq.(11) one may notice identical term to that in Eq. (10) but multiplied by stress dependent function. Eq. (11) reflects experimentally observed fact that void's grow is controlled both by stress and by strain.

σ_m can be computed using Eqs (2) and (8):

$$\sigma_m(Tz=0.5,Q=0) = 0.5[(\sigma_{11}(Q=0))_o + (\sigma_{22}(Q=0))_o] \tag{13}$$

where $$(\sigma_{11}(Q=0))_o = \sigma_o\left(\frac{E}{2\sigma_o}\right)^{\frac{1}{1+n}}\left(\frac{1}{I_n}\right)_o^{\frac{1}{1+n}}(\tilde{\sigma}_{11})_o \tag{14}$$

Similar formula can be written $(\sigma_{22}(Q=0))_o$ changing in Eq. (14) subscripts 11 for 22. For $Tz<0.5$ and $Q\neq 0$ we can write:

$$\sigma_m(Tz<0.5,Q\neq 0) = \frac{(1+Tz)}{3}[\sigma_{11}(Tz<0.5,Q\neq 0)+\sigma_{22}(Tz<0.5,Q\neq 0)] \tag{15}$$

or

$$\sigma_m\left(r=2J/\sigma_o, 0<Tm<0.5, Q\neq 0\right) =$$

$$\frac{(1+Tm)}{3}\sigma_o\left\{\left[(\tilde{\sigma}_{11})_n+(\tilde{\sigma}_{22})_n\right]\left(\frac{E}{2\alpha\sigma_o I_n}\right)_n^{\frac{1}{1+n}}+\left[\begin{array}{l}\left((\tilde{\sigma}_{11})_o+(\tilde{\sigma}_{22})_o\right)\left(\dfrac{E}{2\alpha\sigma_o I_n}\right)_o^{\frac{1}{1+n}}+2Q-\\ +\left((\tilde{\sigma}_{11})_n+(\tilde{\sigma}_{22})_n\right)\left(\dfrac{E}{2\alpha\sigma_o I_n}\right)_n^{\frac{1}{1+n}}\end{array}\right]\left(\frac{Tm}{0.5}\right)^{\alpha 1}\right\} \tag{16}$$

5. Ductile fracture toughness of structural element due to fracture along shear lips

The thinner specimen the greater shear lips widths with respect to the specimen thickness are observed. For sufficiently thin specimens the fractured surface does not contain flat part in between shear lips. In such a case fracture process does not depend on characteristic material length scale (e.g. distance between foreign particles) and depends on characteristic geometrical length scale – in this case, specimen thickness. Fracture mechanisms along shear lips are dominated by plastic shearing strain. Fractured surface along shear lips contains both cavities of elongated parabolic shape and slip facets.

In order to use Eq.(5) we must define J_c^{ds} when fracture takes place along shear lips only. Assume that one can identify the onset of crack growth along the force, P, load point displacement, u, curve. In such a case the critical value of J integral can be, in principle, computed from the well known Rice's formula:

$$J_c = \frac{\eta E}{b_o B} \tag{19}$$

where η depends on specimen shape and size, E is energy of deformation represented by area under the $P=P(u)$ curve at $P=P_{cr}$. $E=E_{el}+E_{pl}$ and $J_c=J_{c,pl}+J_{c,e}$. For some specimens (e.g. SEN(B)) $E_{pl}>>E_{el}$ and E_{el} can be neglected. In such a case one can assume:

$$E_{pl}=V_{pl}\zeta=B^2 b_o \zeta \tag{20}$$

where V_{pl} is volume of plastic deformation domain, ζ is specific energy of shear lips formation, which includes processes of plastic deformation and shear lips formation.

$$J_c^{ds} = \eta B\zeta + J_{c,el} = \eta B\zeta + K_I^2 / E \tag{21}$$

Using the EPRI formula to eliminate the force at the critical moment one can finally reach the following formula for J_c^{ds}, which includes both elastic and plastic parts of energy.

$$J_c^{ds} = \eta B\zeta + \left(\frac{\eta B\zeta}{\alpha \sigma_o \varepsilon_o a} \right)^{\frac{2}{1+n}} \frac{P_o}{b_o B} f(a/W) h_1(a/W, n) \tag{23}$$

where P_o is limit load and $h_1(a/W,n)$ can be found in EPRI report [16]

The unknown ζ, in the analysis to follow will be considered as adjustable parameter and will be selected to make theoretical and experimental results close each other. Nevertheless, ζ is assumed to be constant as in other papers concerning shear lips analysis [11, 12]

For SEN(B) specimen $J_c^{ds} = \eta B\zeta$ =const. It will not depend on specimen thickness unless the thickness is equal or smaller than for purely shear lips fractured surface. Thus, J_c^{ds} will not depend on Tz, unless it can be shown that shear lips covers the whole fractured surface when Tz is still grater than zero. In such a case it can be shown that the formula $J_c^{ds} = const\zeta$ is correct and in this paper we will use: $J_c^{ds} = \eta 0.0025\zeta$

6. Experimental program

The main goal of experimental program was to evaluate fracture toughness of specimens that not follow the standard size limitations. The experimental program was performed on SEN(B) specimens. Width of the specimens W was 25mm. To break the size limitations four different specimen thickness: 4, 6, 12 and 16 mm were selected. For each thickness four different cracks length were machined and prefatigued. The a/W ratio values were: 0.15, 0.35, 0.5, 0.7.

Material used in program was steel 41Cr4 (5140 according to ASTM), which was subjected to two different heat treatments. Mechanical properties of this steel are presented in Table 2.

Table 2. Mechanical properties of 41Cr4 steel.

Material	Label	Heat treatment		Mechanical properties			Ramberg-Ogood parameters	
		Temper	Quench	Re (MPa)	Rm (MPa)	Hardness (HRC)	α	n
40H	A	850^0C	450^0C	1170	1260	44	1	21
40H	B	850^0C	680^0C	700	820	29.5	1	16

7. Numerical computations

Numerical calculations were performed by finite element code ADINA 8.0 system. Material was assumed to be homogeneous with isotropic hardening and satisfying Huber-Mises-Hencky yield criterion. The constitutive relation was assumed as in Eq. 24.

$$\frac{\varepsilon}{\varepsilon_0} = \begin{cases} \sigma/\sigma_0 & for \quad \sigma \le \sigma_0 \\ \alpha(\sigma/\sigma_0)^n & for \quad \sigma > \sigma_0 \end{cases} \tag{24}$$

Stress fields required for Q-stress calculations was obtained using 2-D model with standard 9-nodes elements. 3-D model necessary to obtain *Tz* values was filled with 20-nodes elements. In-plane subdividing of elements was the same as in 2-D case. There were 6 layers in thickness direction. The crack tip was blunted by the radius equal to 10^{-5}m which was 375-1750 times smaller than crack length. The zone next to crack tip was modeled by 16 semi-circles divided on 19 segments. Only one forth of specimen was modeled due to two symmetry axes. Both *Tz* and *Q* were computed at the distance $2J/\sigma_0$ from the crack tip.

8. Results and analysis

In Fig. 2 both experimental and predicted fracture toughness' are presented. Experimental results are shown in the form of unfilled symbols and approximate curves. Computed fracture toughness is shown by filled symbols. They were computed according to presented scheme. Exponent $\alpha 1$ in Eq. (8) was assumed to be 0.1 and specific energy of shear lips formation ζ in Eq. (23) was assumed to be equal to 280 (material A) or to 300 (material B). This quantities require further theoretical and experimental evaluation. Computed and measured quantities are shown also in Table 3.

In the case of material A one may notice a very good agreement between theoretical and measured fracture toughness. Differences do not exceed 10%. For material B maximum difference between computed and measured results is about 25%.

The in-plane constraint strongly influence the fracture toughness. The shorter the crack is the higher values of toughness are observed. For less ductile material these differences are greater. For long cracks (a/W=0.7) the fracture toughness increases over the values measured

and computed for standard specimens. However it is likely that results computed for these specimens are influenced by the action of the contact region.

Also thickness of the specimen (the out of plane constraint) influences fracture toughness (up to 100% for short cracks and material B). The influence is much stronger for short cracks then for long cracks. For short cracks and material B fracture toughness decreases with specimen thickness. For a longer cracks it increases when specimen thickness decreases.

For material A fracture toughness increases when specimen thickness decreases for all crack lengths. However for this material the influence of the specimen thickness on fracture toughness is much less then for material B.

The experimental program and numerical computations were also performed for testing the cleavage fracture toughness on 3H13 steel – Polish Standard (X 30 Cr 13 – DIN; 420 S 45 – BS) tempered 1050^{0}C and quenched 250^{0}C). Good agreement between measured and computed (Eq. 9) results was observed. For cleavage fracture the out-of-plane constraint does not influences fracture toughness essentially. Results will be publish elsewhere because of a limited space in this article.

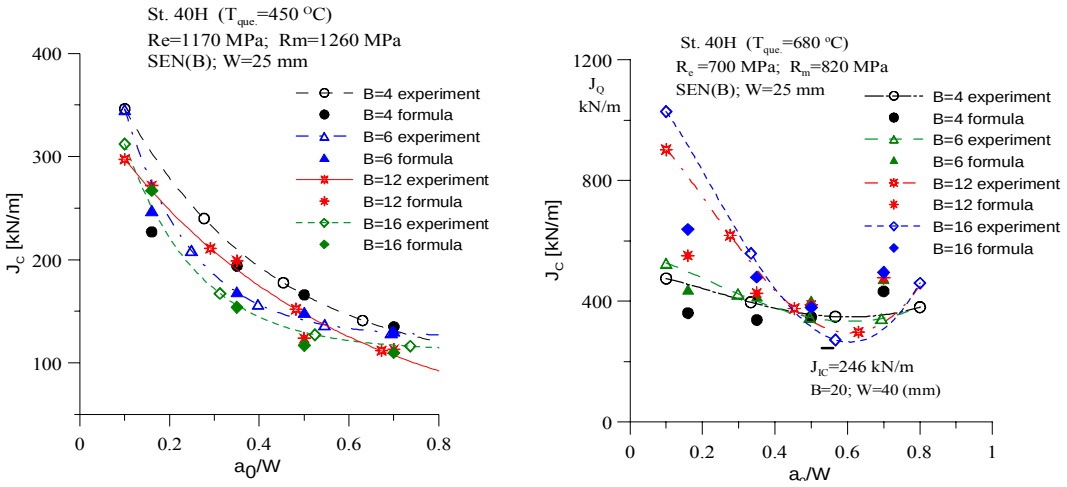

Fig. 2. Comparison of experimental and theoretical fracture toughness

Table 3. Computed and measured fracture toughness values for 41Cr4 quenched at 450^{0}C. (*because of the limited space numerical results are included for one material only*)

	B=4						B=6					
a_o/W	**Jc* exp kN/m**	**Jc* calc kN/m**	A_1mm^2	A_2mm^2	Q	Tz	**Jc exp kN/m**	**Jc calc kN/m**	A_1mm^2	A_2mm^2	Q	Tz
0.16	**303**	**227**	4.32	4.48	-0.86	0.11	**299**	**248**	7.69	4.91	-0.86	0.16
0.35	**200**	**194**	3.58	2.85	-0.48	0.16	**162**	**169**	6.28	3.38	-0.38	0.22
0.50	**165**	**166**	3.25	1.83	-0.28	0.18	**143**	**149**	5.37	2.19	-0.27	0.23
0.70	**128.3**	**135**	2.23	0.82	-0.23	0.21	**111**	**131**	3.72	0.84	-0.23	0.26
	B=12						B=16					
a_o/W	**Jc exp**	**Jc calc**	A_1mm^2	A_2mm^2	Q	Tz	**Jc exp**	**Jc calc**	A_1mm^2	A_2mm^2	Q	Tz

0.16	**266**	**272**	20.84	4.36	-0.83	0.26	**247**	**267**	28	4	-0.82	0.29
0.35	**199**	**199**	16.65	2.55	-0.4	0.27	**155**	**154**	23.12	2.48	-0.37	0.29
0.50	**136**	**124**	13.01	1.87	-0.26	0.29	**121**	**117**	17.8	1.4	-0.25	0.30
0.70	**101**	**113**	6.73	0.47	-0.23	0.30	**117.6**	**110**	8.88	0.72	-0.23	0.31

* average value of 4-6 measurements obtained by drop potential and compliance method

** A_1 an area occupied by voids nucleation-growth-coalescence fracture mechanism, A_2 an area occupied by fracture along shear lips mechanism, $A_1+A_2=Bx0.1b$

References

1. O'Dowd, N.P., Shih, C.F. "Family of crack-tip fields characterized by a triaxiality parameter–I. Structure of fields", *J. Mech. Phys. Solids*, **39**, 8, 989-1015, 1991
2. Hutchinson, J.W., Singular Behaviour at the End of a Tensile Crack in a Hardening Material, *Journal of the Mechanics and Physics of Solids*, **16**, pp.13-31, 1968
3. Guo, W., "Elastoplastic three dimensional crack border field - I. Singular structure of the field", *Engineering Fracture Mechanics,* **46**, 1, 93-104, 1993
4. Guo, W., "Elastoplastic three dimensional crack border field - II. Asymptotic solution for the field", *Engineering Fracture Mechanics*, **46**, 1, 105-13, 1993
5. Guo, W., "Elasto-plastic three-dimensional crack border field - III. Fracture parameters, *Engineering Fracture Mechanics,* **51**, 1, pp.51-71, 1995
6. Neimitz, A., "Dugdale model modification due to the geometry induced plastic constraints", *Engineering Fracture Mechanics*, **67**, 251-61, 2000
7. O'Dowd, N.P., Shih, C.F., "Family of Crack-Tip Fields Characterized by a Triaxiality Parameter – II. Fracture Applications", *J. Mech. Phys. Solids*, **40**, No. 5, pp. 939-963, 1992
8. O'Dowd, N.P. "Application of two parameter approaches in elastic-plastic fracture mechanics", *Engineering Fracture Mechanics,* **52**, 3, 445-465, 1995
9. Gałkiewicz, J., Graba, M., „Algorytm wyznaczania funkcji $\widetilde{\sigma}_{ij}(n,\theta)$, $\widetilde{\varepsilon}_{ij}(n,\theta)$, $\widetilde{u}_i(n,\theta)$, $d_n(n)$, „$I_n(n)$ w rozwiązaniu HRR i jego 3d uogólnieniu, materiały konferencyjne IX Krajowej Konferencji Mechaniki Pękania, Kielce 2003,
10. Kumar, V., German, M.D., Shih, C.F., *An Engineering Approach for Elastic-Plastic Fracture Analysis,* EPRI Report NP-1931, Electric Power Research Institute, Palo Alto, CA, 1981
11. Cheung, S., Luxmoore, A.R., A Shear Lip Analysis of Concave R-Curve for an AlMgZn Alloy, *International Journal of Fracture*, **117**, 195-205, 2002
12. Green, G., Knott, J.K., "On Effects of Thickness on Ductile Crack Growth in Mild Steel", *Journal of the Mechanics and Physics of Solids*, **23**, 167-183, 1975